Cell PRESS
Neuron
Article

Mutant Prion Protein Expression Causes Motor and Memory Deficits and Abnormal Sleep Patterns in a Transgenic Mouse Model

Sara Dossena,[1,2,8] Luca Imeri,[4,8] Michela Mangieri,[5] Anna Garofoli,[1,2] Loris Ferrari,[1,4] Assunta Senatore,[1,2] Elena Restelli,[1,2] Claudia Balducci,[2] Fabio Fiordaliso,[3] Monica Salio,[3] Susanna Bianchi,[4] Luana Fioriti,[1,2,9] Michela Morbin,[5] Alessandro Pincherle,[6] Gabriella Marcon,[5,7] Flavio Villani,[6] Mirjana Carli,[2] Fabrizio Tagliavini,[5] Gianluigi Forloni,[2] and Roberto Chiesa[1,2,*]

[1]Dulbecco Telethon Institute, 20156 Milan, Italy
[2]Department of Neuroscience
[3]Bio-imaging Unit, Department of Cardiovascular Research
"Mario Negri" Institute for Pharmacological Research, 20156 Milan, Italy
[4]Department of Human Physiology, University of Milan Medical School, 20133 Milan, Italy
[5]Division of Neuropathology and Neurology
[6]Division of Clinical Epileptology and Experimental Neurophysiology
"Carlo Besta" National Neurological Institute, 20133 Milan, Italy
[7]Department of Pathology and Experimental Medicine, University of Udine, 33100 Udine, Italy
[8]These authors contributed equally to this work
[9]Present address: Department of Neuroscience, Columbia University, New York, NY 10032, USA
*Correspondence: chiesa@marionegri.it
DOI 10.1016/j.neuron.2008.09.008

SUMMARY

A familial form of Creutzfeldt-Jakob disease (CJD) is linked to the D178N/V129 prion protein (PrP) mutation. Tg(CJD) mice expressing the mouse homolog of this mutant PrP synthesize a misfolded form of the mutant protein, which is aggregated and protease resistant. These mice develop clinical and pathological features reminiscent of CJD, including motor dysfunction, memory impairment, cerebral PrP deposition, and gliosis. Tg(CJD) mice also display electroencephalographic abnormalities and severe alterations of sleep-wake patterns strikingly similar to those seen in a human patient carrying the D178N/V129 mutation. Neurons in these mice show swelling of the endoplasmic reticulum (ER) with intracellular retention of mutant PrP, suggesting that ER dysfunction could contribute to the pathology. These results establish a transgenic animal model of a genetic prion disease recapitulating cognitive, motor, and neurophysiological abnormalities of the human disorder. Tg(CJD) mice have the potential for giving greater insight into the spectrum of neuronal dysfunction in prion diseases.

INTRODUCTION

Clinical signs in the diagnosis of prion diseases in animal models are essentially confined to late motor deficits. In humans, prion diseases have a more complex presentation, with dementia and nonmotor as well as motor disturbances, often following a long prodromal phase. A broader spectrum of clinical signs is needed in experimental models for insight into the mechanisms of neuronal dysfunction and its evolution, and to identify earlier markers of clinical disease when therapeutic intervention may be effective. Here we report the emergence of behavioral, electrophysiological, and motor deficits in a mouse model of inherited prion disease that closely mirror those seen in a newly diagnosed human patient with the same mutation.

Approximately 15% of human prion diseases display autosomal dominant inheritance and are linked to point or insertional mutations in the gene encoding PrP^{C} (*PRNP*) (Young et al., 1999). The mechanism of neurotoxicity of mutant PrP molecules is not clear (Chiesa and Harris, 2001), but structural changes involving increased β sheet structure, aggregation, and resistance to protease digestion may contribute to the pathogenicity of the mutant protein (Prusiner, 1998). *PRNP* mutations have been associated with defined clinical and neuropathological phenotypes—Creutzfeldt-Jakob disease (CJD), Gerstmann-Sträussler-Scheinker syndrome (GSS), and fatal familial insomnia (FFI)—but there is extensive variability in disease presentation for individual mutations and even within the same family (Young et al., 1999).

An important source of phenotypic variation is the polymorphism at codon 129 of *PRNP*, where either methionine (M) or valine (V) can be encoded. The prion disease linked to the substitution of aspartic acid (D) to asparagine (N) at codon 178 is a typical example. The D178N/V129 haplotype segregates with a subtype of Creutzfeldt-Jakob disease (CJD^{178}) recognized clinically by global cortical dementia, motor abnormalities, and myoclonus, whereas the D178N/M129 allele is associated with FFI, primarily characterized by severe sleep alterations, with total disorganization of normal sleep structure and endocrine dysfunction (Goldfarb et al., 1992). Electroencephalographic (EEG) changes

characterize CJD (Wieser et al., 2006). However, sleep alterations are also increasingly recognized in sporadic and inherited CJD (Calleja et al., 1985; Chapman et al., 1996; Kazukawa et al., 1987; Landolt et al., 2006; Taratuto et al., 2002; Terzano et al., 1995).

Investigation of inherited prion disease biology requires animal models with the essential features of the human disorders. To date, the existing mouse models of inherited human prion disease, Tg(P101L) (Hsiao et al., 1990; Nazor et al., 2005; Telling et al., 1996) and Tg(PG14) (Chiesa et al., 1998), develop motor deficits, but models showing the cognitive and neurophysiological abnormalities typical of CJD have not been reported.

Here we describe a transgenic mouse model of inherited CJD expressing the mouse homolog of the D178N/V129 mutation, in which we found EEG and sleep abnormalities as well as memory impairment and motor dysfunction. Striking morphological alterations of the neuronal endoplasmic reticulum (ER) associated with ER retention of mutant PrP were found in these animals, suggesting that perturbation of ER homeostasis may be involved in the pathogenesis. These mice increase the spectrum of clinical signs and other functional abnormalities in experimental models of prion disease. They provide a platform for greater insight into mechanisms of disease pathogenesis and for potential approaches to intervention.

RESULTS

Generation of Transgenic Mice and Characterization of Mutant PrP

We produced transgenic mice that express a mouse PrP (moPrP) homolog of the D178N/V129 mutation associated with CJD[178] (moPrP D177N/V128). We identified five founders (A21, G1, G5, H, and I). Transgene copy number and mutant PrP expression are shown in Table S1 and Figure S1 in the Supplemental Data available online. To generate transgenic lines, referred to as Tg(CJD), founders were bred with *Prnp*$^{0/0}$ mice (Bueler et al., 1992), so that the progeny expressed only mutant PrP. The pattern of transgenic PrP expression in the brain was similar to that of endogenous PrP in nontransgenic mice (Figure S2), although subtle differences in cellular distribution cannot be excluded. Unglycosylated PrP was underrepresented (Figures S1 and S2A), consistent with observations in humans carrying the D178N mutation (Petersen et al., 1996).

Approximately 50% of mutant PrP in the mouse brains was insoluble (seen in pellet fractions in Figures 1A and 1B and Figure S3) and was immunoprecipitated by the PrP^{Sc}-specific antibody 15B3, which also recognizes a variety of misfolded and aggregated forms of PrP (Biasini et al., 2008; Nazor et al., 2005) (Figure 1B). No detergent-insoluble PrP was detected in nontransgenic mice (Figure 1A, lanes 1 and 2).

Mutant PrP was weakly protease resistant (Figure 1C, lanes 5–12), in contrast to the complete protease sensitivity of wild-type PrP (Figure 1C, lanes 1–4). This was clearly seen under standard assay conditions in the Tg(CJD-G5) founder expressing high levels of mutant PrP. To enhance detection of the proteinase K (PK)-resistant fraction in Tg(CJD-A21) mice, brain homogenates were digested at 4°C (Figure 1D). After deglycosylation with PNGase F, the PK-resistant fragment found in Tg(CJD) mice had an apparent molecular mass of 19 kDa (Figure 1E). There were no regional differences in insolubility and protease resistance of mutant PrP throughout the brain (Figure S3 and data not shown).

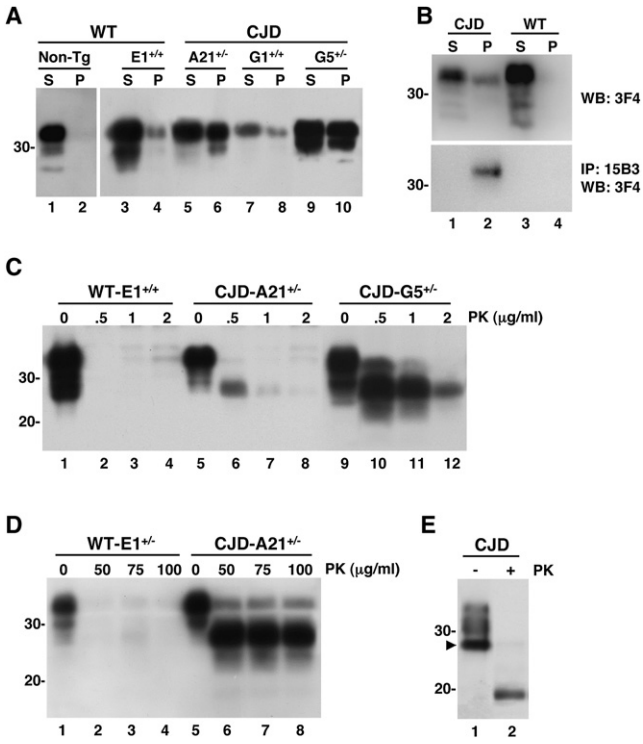

Figure 1. D177N/V128 PrP is Insoluble, Immunoprecipitated by 15B3 Antibody, and Mildly Protease Resistant

(A) Brain lysates prepared from mice of the following genotypes and ages were ultracentrifuged at 186,000 × g for 40 min, and PrP in the supernatants (S) and pellets (P) was analyzed by western blotting using P45–66 (lanes 1 and 2) or 3F4 antibody (lanes 3–10): non-Tg/*Prnp*$^{+/+}$, 304 days (lanes 1 and 2); Tg(WT-E1$^{+/+}$), 581 days (lanes 3 and 4); Tg(CJD-A21$^{+/-}$), 570 days (lanes 5 and 6); Tg(CJD-G1$^{+/+}$), 309 days (lanes 7 and 8); Tg(CJD-G5$^{+/-}$)/*Prnp*$^{+/+}$, 72 days (lanes 9 and 10).

(B) Brain lysates from Tg(CJD-A21$^{+/-}$), 720 days (lanes 1 and 2) and Tg(WT-E1$^{+/+}$), 581 days (lanes 3 and 4) were ultracentrifuged, and the supernatant and pellet fractions were split into two parts and either analyzed by western blotting using antibody 3F4 (top panel) or immunoprecipitated using monoclonal antibody 15B3 (lower panel). Immunoprecipitated PrP was analyzed by western blotting using antibody 3F4 (lower panel).

(C) Brain lysates from mice of the following genotypes and ages were incubated with 0–2 μg of proteinase K (PK) for 30 min at 37°C, and PrP was visualized by western blotting using antibody 3F4: Tg(WT-E1$^{+/+}$), 42 days (lanes 1–4); Tg(CJD-A21$^{+/-}$), 153 days (lanes 5–8); Tg(CJD-G5$^{+/-}$)/*Prnp*$^{+/+}$, 72 days (lanes 9–12). The undigested samples (0 μg/ml PK) represent 50 μg of protein; the other samples represent 200 μg.

(D) Brain lysates from a 71-day-old Tg(WT-E1$^{+/-}$) mouse and a 191-day-old Tg(CJD-A21$^{+/-}$) mouse were incubated with 0–100 μg of PK for 60 min on ice, and PrP was visualized by western blotting with antibody 3F4. The undigested samples (0 μg/ml PK) represent 5 μg of protein; the other samples represent 20 μg.

(E) Brain lysate from a 422-day-old Tg(CJD-A21$^{+/-}$) mouse was incubated with 0 or 75 μg/ml of PK as in (D), followed by incubation with PNGase F and western blot analysis with antibody 3F4. Deglycosylation of the undigested sample in lane 1 was incomplete; arrowhead indicates the completely deglycosylated PrP band.

A

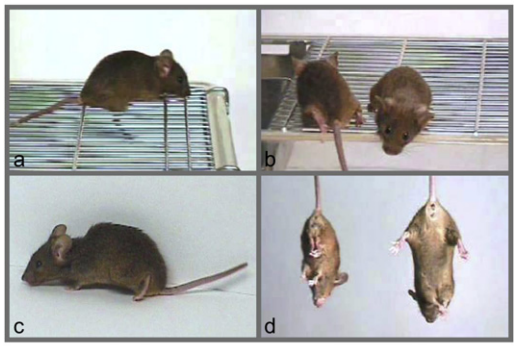

B

Clinical Illness in Tg(CJD) mice

	Hemizygous		Homozygous	
Age at Onset	452 ± 15	(67)	144 ± 7	(20)
Age at Death	704 ± 26	(34)	284 ± 11	(19)
Duration of Illness	293 ± 28	(31)	130 ± 13	(13)

Mean number of days ± SEM. The number in each group is given in parentheses.

Figure 2. Neurological Symptoms in Tg(CJD) Mice

(Aa) A Tg(CJD-A21$^{+/+}$) mouse at 201 days of age is incapable of deambulating on a metal grill.

(Ab) Two Tg(CJD-A21$^{+/+}$) mice at 201 and 223 days of age. Note the ataxic posture with extension of the hindlimb and the unbalanced posture.

(Ac) A Tg(CJD-A21$^{+/-}$) mouse at 671 days of age shows kyphosis (hunchback position) and abnormal gait with extension of the hindlimbs.

(Ad) When suspended by its tail, a Tg(CJD-A21$^{+/+}$) mouse at 188 days of age (left) assumes a flexed posture and tightly clasps its hindlimbs, whereas a nontransgenic littermate (right) splays its limbs.

(B) Time course of clinical illness in Tg(CJD-A21) mice.

Tg(CJD) Mice Develop Motor Dysfunction and Alteration of Spatial Working Memory

All Tg(CJD) mice expressing mutant PrP at a level similar to that of endogenous PrP in wild-type mice, or higher, exhibited progressive neurological disease. They developed ataxia, with abnormal posture, leaning to one side, unusual flexed posture of hind legs, kyphosis, and foot clasping on suspension (Figure 2A). On a rotarod, Tg(CJD) mice showed a significantly shorter latency to fall than *Prnp*$^{+/+}$ or *Prnp*$^{0/0}$ nontransgenic littermates and Tg(WT) mice (Figure S4).

The phenotype was evident from ~450 days in hemizygous Tg(CJD-A21) mice and ~145 days in homozygous mice. Duration of illness was 293 ± 28 and 130 ± 13 days (Figure 2B), respectively, suggesting a transgene dose-related neurological dysfunction. Furthermore, the Tg(CJD-G5) founder, which expressed mutant PrP at eight times wild-type levels, died with neurological symptoms at 72 days of age, whereas mice expressing mutant PrP below the endogenous level did not develop neurological disease during their lifetimes. Nontransgenic littermates and Tg(WT) mice observed over the same period remained free of neurological disease and survived more than 1000 days.

Coexpression of wild-type PrP had no effect on onset, severity, or duration of illness in Tg(CJD) mice, in contrast to the effect of endogenous PrP expression in other transgenic mutant PrP models (Telling et al., 1996). For example, in a group of littermates consisting of 10 Tg(CJD-A21$^{+/-}$)/*Prnp*$^{+/+}$, 13 Tg(CJD-A21$^{+/-}$)/*Prnp*$^{+/0}$, and 7 Tg(CJD-A21$^{+/-}$)/*Prnp*$^{0/0}$ mice, symptom onset was at 405 ± 44, 409 ± 35, and 410 ± 39 days, respectively (mean ± SEM).

A

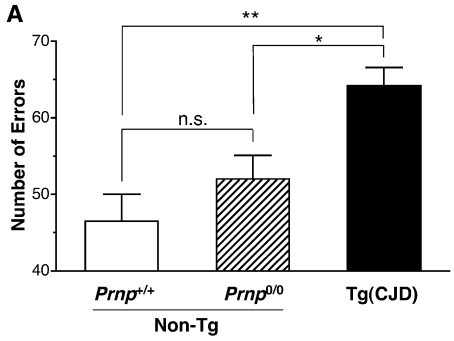

B

Mouse Line	Latency (sec)
Non-Tg/*Prnp*$^{+/+}$	232.8 ± 24.9
Non-Tg/*Prnp*$^{0/0}$	317.0 ± 34.1
Tg(CJD)	248.6 ± 19.4

Figure 3. Tg(CJD) Mice Show Working Memory Impairment in the Eight-Arm Radial Maze

(A) Histograms show the mean ± SEM of total errors in the eight-arm radial maze during 10 days of training by 10 non-Tg/*Prnp*$^{+/+}$, 10 non-Tg/*Prnp*$^{0/0}$, and 11 Tg(CJD-A21$^{+/-}$) mice aged between 200 and 316 days. $F_{2,28}$ = 9.0; p = 0.001 by one-way analysis of variance (ANOVA). *p < 0.05, **p < 0.01 by Tukey's post hoc test.

(B) Values show the mean latency (±SEM) to complete the test. One-way ANOVA did not find any difference between groups ($F_{2,28}$ = 2.8; p = 0.08).

We also found alterations in spatial working memory in Tg(CJD) mice. Mice were tested with a battery of behavioral tasks for different aspects of memory, including passive avoidance, novel object recognition, Morris water maze, and eight-arm radial maze. To avoid confounding effects due to the motor deficit that develops in older mice, we tested Tg(CJD) hemizygous animals younger than 320 days. Mice performed poorly in the eight-arm radial maze, which tests spatial working memory, making significantly more errors over 10 training days than nontransgenic controls (Figure 3A). Latency to complete the test was similar in Tg(CJD) and control mice, confirming that the deficit was not due to motor abnormalities (Figure 3B). We found no significant differences between Tg(CJD) and control mice in the other behavioral tasks at this stage.

Tg(CJD) Mice Show Abnormal EEG Patterns and Sleep Disturbance Reminiscent of Those Observed in a Human CJD Patient with the Same Mutation

As EEG abnormalities are common in CJD (Wieser et al., 2006), we analyzed EEG patterns in Tg(CJD) mice. The EEG activity of Tg(CJD) mice was characterized by bursts of polyphasic complexes (Figure 4A, left panels), which were not seen in the other groups of mice. The polyphasic complexes lasted from 0.3 to 4.6 s, and their amplitude varied but in most cases was larger than the EEG amplitude during non-REM (NREM) sleep. The frequency power spectrum of polyphasic complexes peaked

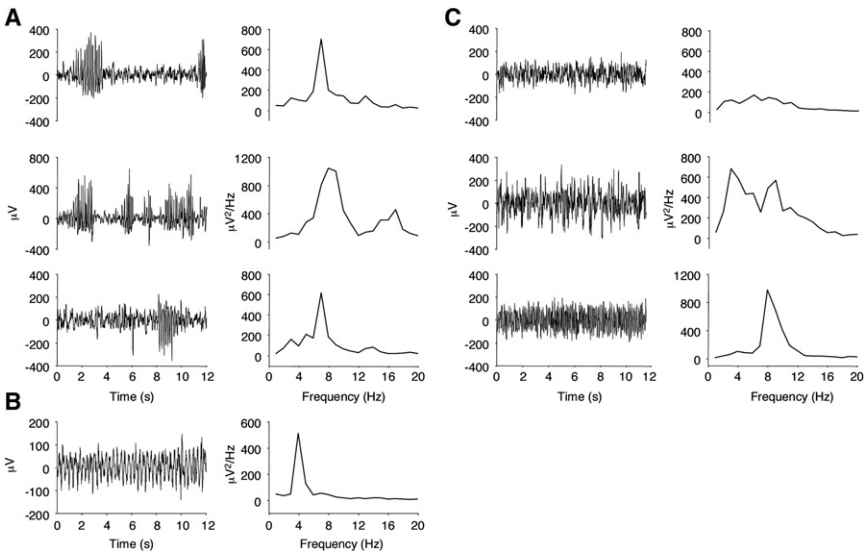

Figure 4. Electroencephalographic Activity Is Altered in Tg(CJD) Mice

(A) Three examples of bursts of polyphasic complexes (left panels) and corresponding frequency power spectra obtained by fast Fourier transform (right panels). These alterations were observed in all 6 Tg(CJD-A21$^{+/-}$) mice.

(B) An example of sawtooth waves (left panel) and the corresponding frequency power spectrum (right panel), which were observed in 5 out of 6 Tg(CJD-A21$^{+/-}$) mice.

(C) Examples of normal electroencephalographic recordings (left panels) and corresponding frequency power spectra (right panel) during epochs of wakefulness (top panel), non-rapid eye movement (NREM) (middle panel), and rapid eye movement (REM) (bottom panel) sleep in a representative Tg(WT) mouse.

around 7–8 Hz (Figure 4A, right panels). Scoring epochs (12 s) containing one or more bursts of polyphasic complexes were almost equally distributed during the light and dark phases (33.0% ± 5.5% and 27.8% ± 5.6% of the total number of epochs, respectively). During the light phase, polyphasic complexes were present in 36.1% ± 4.8%, 18.7% ± 4.0%, and 13.8% ± 7.4% of epochs scored as wakefulness, NREM sleep, and REM sleep, respectively. These percentages were 29.7% ± 4.4%, 29.3% ± 2.9%, and 13.6% ± 11.3% during the dark phase. As shown in the lower panel of Figure 5B, the polyphasic complexes were distributed in clusters.

In 5 out of 6 Tg(CJD) mice, we also observed abnormal "sawtooth" waves with a frequency power spectrum that peaked around 4 Hz (Figure 4B). The number of epochs with these waves ranged from 5 to 33 during the light phase and from 4 to 56 during the dark phase, except in one Tg(CJD) mouse in which hundreds of sawtooth waves were recorded during the light-dark cycle.

Mice expressing mutant PrP showed marked sleep abnormalities; 24 hr polygraphic analysis indicated significant alterations of sleep-wake patterns. Tg(CJD) mice spent strikingly less time in REM sleep than all other mouse lines during both phases of the light-dark cycle (Figure 5A; top panel of Figure 5B; Figure 5E; Figure S5). The amount of time spent in NREM sleep during the dark phase was also significantly reduced. In Tg(CJD) mice, 3.9% ± 2.1% of time during the light phase and 4.7% ± 1.9% during the dark phase was characterized by repeated bursts of polyphasic complexes and could not be assigned to any conventional behavioral state; these periods were classified as "unscored" (Figure 5B, top panel). There were no significant differences in the number of transitions between behavioral states (an indicator of continuous or broken sleep) or state-specific EEG power spectra in the different groups of mice.

Analysis of circadian distribution of sleep and gross body movements did not bring to light any differences between Tg(CJD) and control mice. As expected in nocturnal animals, mice of all experimental groups spent more time awake (Figure 5E, top panel) and moved more during the dark phase than the light phase of the light-dark cycle, with no differences between strains (F_3 = 0.64, p = 0.6 by two-way ANOVA). Animals of all strains also slept more (as evaluated by total sleep time) during the light phase than the dark phase. Thus, the extreme reduction of REM sleep in Tg(CJD) mice could not be attributed to alterations of circadian rhythms.

Our findings of marked EEG and sleep disruption in Tg(CJD) mice expressing the mouse homolog of the D178N/V129 mutation confirm that sleep dysfunction is more widespread in prion diseases than previously thought, consistent with recent reports of such disturbances not only in FFI (Landolt et al., 2006). We therefore examined the sleep profile and EEG of a case of CJD^{178} in a 47-year-old woman newly diagnosed during the course of our experiments (see case report in the Supplemental Data).

We found EEG alterations (periodic sharp wave complex [PSWC] activity) and marked abnormalities in the patient's sleep profile. NREM sleep EEG pattern was characterized by monomorphic low-amplitude theta and unstable delta activities, with total absence of vertex waves, spindles, and K complex. Triphasic waves were clearly attenuated during NREM sleep. REM sleep, limited to brief phases during the night, appeared characterized by very low-amplitude theta and beta rhythms, reduction of submental electromyographic tone, and only rare rapid eye movements (Figure S6). These severe EEG alterations meant that the sleep-wake profile could not be scored according to Rechtschaffen and Kales (1968). However, we identified three patterns on the basis of the above characteristics: wake, NREM sleep, and REM sleep (Figure 5D). Sleep appeared very unstable, with frequent transitions between wakefulness and NREM sleep. NREM sleep was also broken by frequent arousals associated with limb movements (limb movement index = 64). The respiratory profile was unremarkable.

In summary, some of the neurophysiological features of Tg(CJD) mice are similar to those observed in the CJD^{178} patient.

Tg(CJD) Mice Show PrP Deposits, Gliosis, and Loss of GABAergic Cells

Tg(CJD) mice exhibited several neuropathological abnormalities. Immunohistochemistry indicated protease-resistant PrP

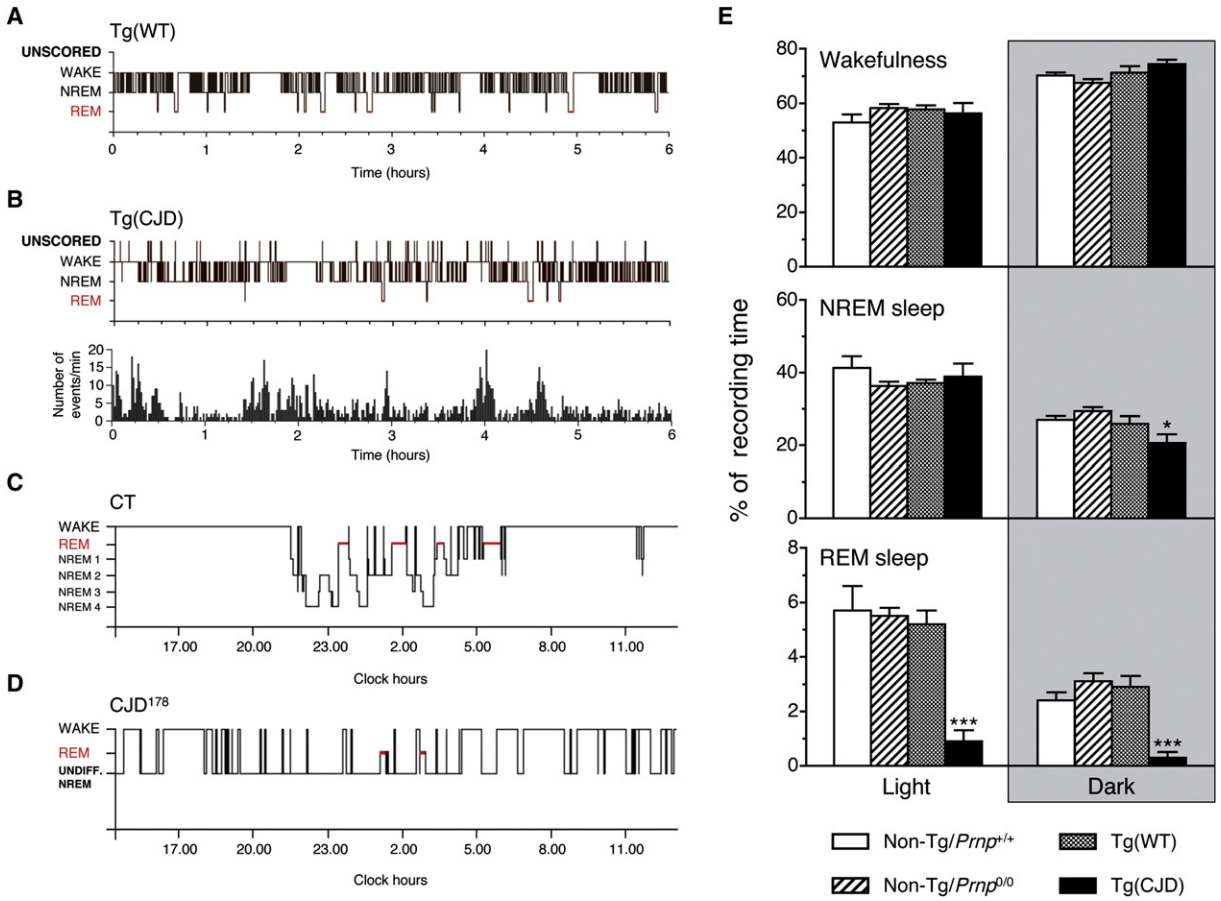

Figure 5. Abnormal Sleep Patterns in Tg(CJD) Mice and a Human CJD^{178} Patient

(A) Representative hypnogram of a 578-day-old Tg(WT-E1$^{+/+}$) mouse. "Unscored" indicates epochs not assigned to any behavioral state. (See Results and Experimental Procedures for further details.)

(B) Representative hypnogram (upper panel) and distribution across time of polyphasic complexes (lower panel) in a 631-day-old Tg(CJD-A21$^{+/-}$) mouse. Note the reduction in REM sleep epochs (highlighted in red) in comparison to the Tg(WT-E1$^{+/+}$) mouse and the presence of unscored epochs. Hypnograms in (A) and (B) cover the first 6 hr of the light phase of the light-dark cycle and are intended to provide a qualitative picture of the amount of sleep and sleep distribution in time (sleep architecture) during this interval.

(C) The 24 hr hypnogram of a healthy human shows a normal pattern of waking during the daytime and regular NREM-REM cycles during the night.

(D) Only a rudimentary wake-sleep rhythm is detectable in a human patient carrying the D178N/V129 PrP mutation, with a prevalence of waking during the day and sleep epochs during the night. Note the absence of ultradian cycles, the severe reduction of REM sleep, and the impossibility to distinguish NREM sleep stages.

(E) Percentage of time (mean ± SEM) spent in wakefulness, NREM sleep, and REM sleep across 24 hr by 6 non-Tg/*Prnp*$^{+/+}$, 6 non-Tg/*Prnp*$^{0/0}$, 6 Tg(CJD-A21$^{+/-}$), and 5 Tg(WT-E1$^{+/+}$) mice. At the time of recording, the animals' mean (±SEM) ages were: non-Tg/*Prnp*$^{+/+}$, 629 ± 20 days; non-Tg/*Prnp*$^{0/0}$, 632 ± 59 days; Tg(WT-E1$^{+/+}$), 427 ± 70 days; Tg(CJD-A21$^{+/-}$), 560 ± 34 days. The gray background identifies the dark portion of the light-dark cycle. Two-way ANOVA indicated a significant reduction in the percentage of time spent in REM sleep during both the light and dark phases for the Tg(CJD) animals ($F_{3,42}$ = 4.8, p = 0.01). *p < 0.05, ***p < 0.001 versus other groups by Fisher's test.

deposits in many brain regions of Tg(CJD) mice that were absent in nontransgenic and Tg(WT) mice (Figures 6A–6D). Diffuse "synaptic-type" PrP deposition was prominent in the hippocampal formation, particularly in the stratum moleculare (Figure 6E), and in the amygdala and olfactory bulb. Definite PrP immunostaining was also detected in the neocortex and striatum and, less intensely, in the thalamus, hypothalamus, brainstem, and molecular layer of the cerebellum. In addition, small PrP "plaque-like" deposits were found in several brain regions, including the fimbria of the hippocampus, the reticular thalamic nucleus, the corpus callosum, the external and internal capsule, the cingulate cortex, and the anterior commissure nuclei (Figure 6F). These deposits were not fluorescent after thioflavine S staining, indicating that they did not contain amyloid fibrils.

PrP deposition was associated with hypertrophy and proliferation of astrocytes, prominent in the hippocampus, amygdala, and olfactory bulb as revealed by immunostaining with anti-glial fibrillary acidic protein (GFAP) antibody (Figure S7). No spongiform-like changes were observed.

There is evidence that parvalbumin-, calbindin-, and calretinin-positive subpopulations of GABAergic neurons are primarily affected in CJD (Belichenko et al., 1999; Guentchev et al., 1997). Immunohistochemistry for calretinin showed striking differences in the hippocampus and cerebral cortex of Tg(CJD) mice

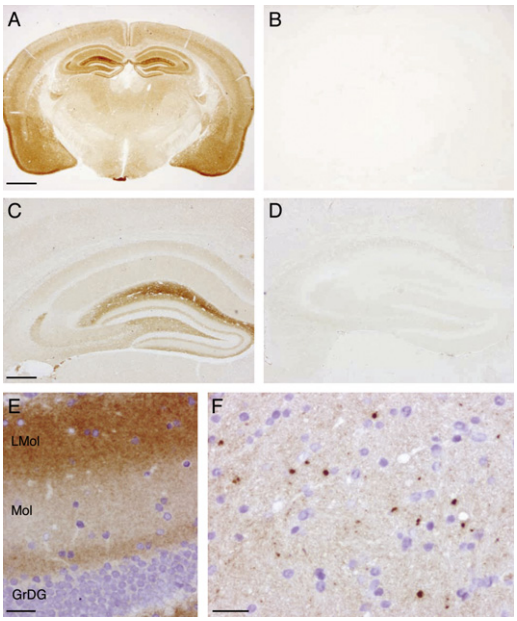

Figure 6. Tg(CJD) Mice Show Cerebral Accumulation of Protease-Resistant PrP

(A and B) Immunohistochemical detection of PrP using monoclonal antibody 12B2 after PK digestion of a section in a 290-day-old Tg(CJD-A21$^{+/+}$) mouse (A) and a 396-day-old non-Tg/*Prnp*$^{+/+}$ mouse (B).

(C and D) Immunohistochemical detection of PrP using monoclonal antibody 3F4 after PK digestion of a section in a 267-day-old Tg(CJD-A21$^{+/+}$) mouse (C) and a 293-day-old Tg(WT-E1$^{+/-}$) mouse (D).

(E and F) The pattern of PrP deposition in Tg(CJD) mice was either diffuse, as in the hippocampal formation (E), or plaque-like, as in the anterior commissure nucleus (F). Sections in (E) and (F) are from a 744-day-old Tg(CJD-A21$^{+/-}$) mouse.

Scale bars = 1 μm in (A) (also applicable to [B]), 250 μm in (C) (also applicable to [D]), and 25 μm in (E) and (F). Lmol, lacunosus molecular stratum; Mol, molecular stratum; GrDG, granular zone of dentate gyrus.

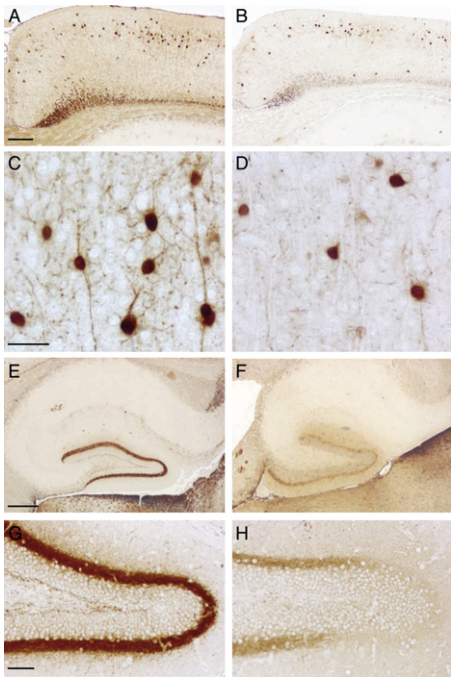

Figure 7. Tg(CJD) Mice Show Low Calretinin Immunoreactivity in Several Nerve Cell Populations

Sections from non-Tg/*Prnp*$^{0/0}$ mice aged 245 (A and C), 334 (E), or 808 (G) days; Tg(CJD-A21$^{+/+}$) mice aged 284 (B and D) or 208 (F) days; and a 709-day-old Tg(CJD-A21$^{+/-}$) mouse (H) were stained with anti-calretinin antibody. In non-Tg mice, calretinin immunostaining labels bipolar and multipolar neurons in layers II and III of the cerebral cortex (A and C) and the synaptic terminals of the mossy cells in the supragranular zone of the dentate gyrus in the hippocampus (E and G). Tg(CJD) mice show marked loss of calretinin immunoreactivity in cortical neurons (B and D) and hippocampal mossy cell terminals (F and H). Scale bars = 250 μm in (A) and (E) (also applicable to [B] and [F]), 15 μm in (C) (also applicable to [D]), and 50 μm in (G) (also applicable to [H]).

compared to controls (Figure 7; Figure S8). In non-Tg mice, the anti-calretinin antibody strongly labeled bipolar neurons in layers II and III of the cerebral cortex, mossy cells in the dentate gyrus of the hippocampus, and their synaptic terminals projecting to the supragranular zone. Tg(CJD) mice consistently showed markedly less calretinin immunoreactivity of interneurons and neuropil of the cerebral cortex and mossy cell terminals in the hippocampus. The loss of calretinin immunoreactivity progressed with age and correlated with the local deposition of PrP, although the two proteins did not colocalize precisely (Figure S8). Synaptophysin immunoreactivity was low in the supragranular layer of the hippocampus where calretinin reduction was most pronounced (data not shown).

These observations indicate a profound abnormality of calretinin-positive fibers at the synaptic terminals up to their complete disappearance.

Tg(CJD) Cerebellar Granule Neurons Show Swelling of the ER and Abnormal Intracellular Localization of PrP

Histological analysis of Tg(CJD) brains did not find any obvious signs of cerebellar degeneration, in contrast to other transgenic mutant PrP models with similar motor dysfunctions (Chiesa et al., 1998, 2000). Tg(CJD) cerebella were not atrophic judging from morphometric measurements, nor did they show loss of granule neurons or alterations of Purkinje cell density and dendritic arborization in the molecular layer (Figure S9; data not shown). Electron microscopy of Tg(CJD) cerebella, however, detected striking ultrastructural abnormalities in granule neurons. The ER of these cells was consistently enlarged and fragmented (Figure 8A). These abnormalities were not seen in non-Tg/*Prnp*$^{0/0}$ or Tg(WT) mice, suggesting that they were related to mutant PrP expression.

To test whether the ultrastructural alterations were associated with accumulation of mutant PrP in the secretory pathway, we used immunogold electron microscopy. Because immunostaining of mutant PrP in brain sections requires antigen retrieval with guanidine thiocyanate, which alters the tissue ultrastructure, we made this analysis in primary cerebellar cultures established from newborn mice. Preliminary tests showed that mutant PrP could in fact be detected in paraformaldehyde/glutaraldehyde-fixed neurons without the need for antigen retrieval. The majority of wild-type PrP in granule neurons from non-Tg/*Prnp*$^{+/+}$ and Tg(WT) mice localized on the plasma membrane and in endosomes, with only a small fraction in the ER and the Golgi

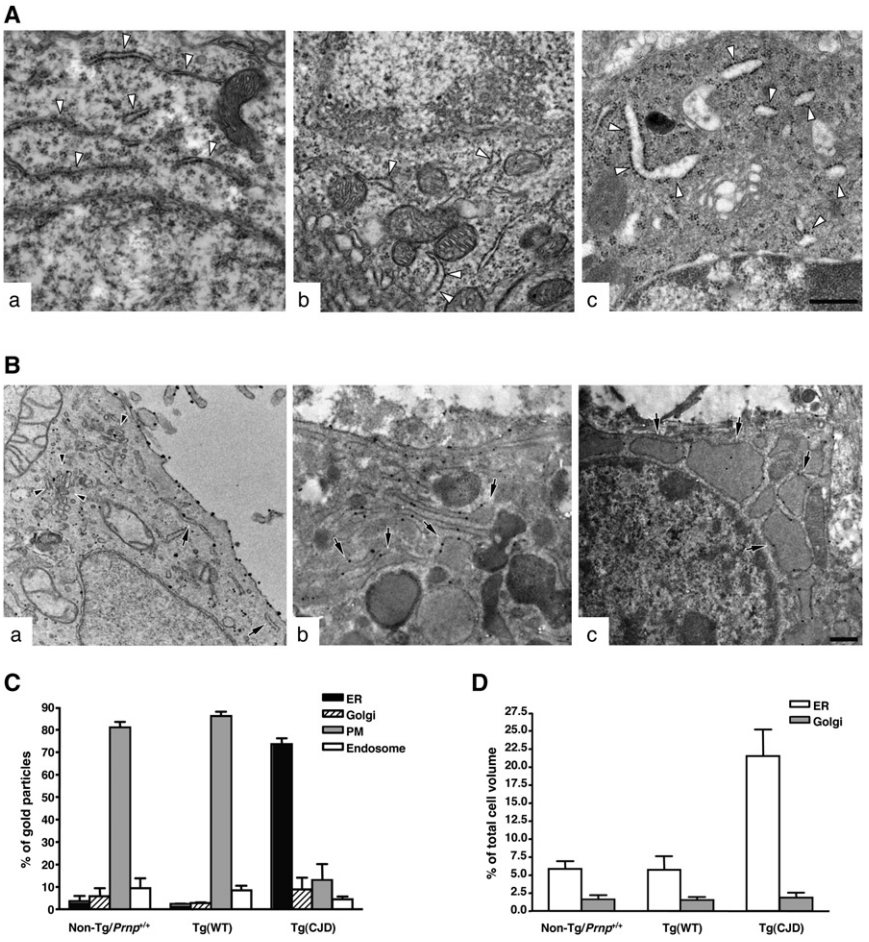

Figure 8. Tg(CJD) Neurons Have Enlarged Endoplasmic Reticulum and Abnormal Intracellular PrP Distribution

(A) Electron microscopy of granule neurons in the cerebellum of a 268-day-old non-Tg/*Prnp*$^{0/0}$ mouse (Aa), a 262-day-old Tg(CJD-A21$^{+/-}$) mouse (Ab), and a 43-day-old Tg(CJD-A21$^{+/+}$) mouse (Ac). Arrowheads point to the endoplasmic reticulum (ER) cisternae, which are normal in the non-Tg control (Aa) mouse but are fragmented and swollen in the Tg(CJD) mice (Ab and Ac). Scale bar in (Ac) (applicable to [Aa]–[Ac]) = 500 nm.

(B) Cultures of cerebellar granule neurons from non-Tg/*Prnp*$^{+/+}$, Tg(WT), and Tg(CJD-A21$^{+/-}$) mice were fixed and labeled with anti-PrP antibody using the Nanogold enhancement protocol. Wild-type PrP is mostly found at the plasma membrane (Ba); some staining is also visible in the ER (arrows) and in the Golgi complex (arrowheads). D177N/V128 PrP is mostly found in ER cisternae, which appear moderately (Bb) or strongly (Bc) enlarged and swollen. Scale bar in (Bc) (applicable to [Ba]–[Bc]) = 250 nm.

(C) Quantification of gold particles in different cell compartments. PM, plasma membrane.

(D) Quantification of ER and Golgi volumes of cultured cerebellar granule neurons.

Data are the mean ± SD of at least 10 cells per specimen.

complex (Figures 8Ba and 8C). In contrast, mutant PrP localized mostly in the ER of Tg(CJD) neurons (~75% versus ~2.5% in control cells), with a much smaller fraction of molecules on the plasma membrane (~15% versus ~85% in controls) (Figures 8Bb, 8Bc, and 8C). Cultured cerebellar neurons from the mutant mice showed striking alterations of the ER cisternae, which appeared enlarged, swollen, and electron-dense (Figures 8Bb, 8Bc, and 8D).

These results indicate altered trafficking of mutant PrP to the plasma membrane, protein retention in the ER, and morphological abnormalities in intracellular organelles.

DISCUSSION

The D178N/V129 haplotype is linked to a CJD subtype that has been described in families from Germany, France, Finland, Israel, and America (Young et al., 1999). The disease is characterized by early cognitive impairment with prominent memory deterioration, abnormal behavior, and progressive signs of motor dysfunction such as ataxia, tremor, and myoclonus, as well as characteristic neuropathological signs. In the present study, we found that mice carrying a transgene encoding the mouse homolog of the CJD^{178} mutation accumulate an abnormal form of PrP in their brains and show neuropathological changes of prion diseases. We also found that the mutant mice develop a neurological illness characterized by progressive motor dysfunction, deficits in spatial working memory, and abnormal sleep-wake behavior with dramatic reduction of REM sleep. Although sleep abnormalities are not commonly considered symptoms of CJD^{178}, we have now reported sleep disorganization with severe reduction of REM epochs in a recently diagnosed patient with the D178N/V129 mutation. Thus, our combined behavioral and neurophysiological analyses indicate that Tg(CJD) mice recapitulate essential clinical features of CJD^{178}. The results also suggest that perturbation of ER homeostasis due to mutant PrP misfolding may be a critical factor in neuronal dysfunction in inherited prion disease, indicating new pathogenic mechanisms and potential therapeutic strategies.

Clinical Features of Tg(CJD) Mice

Tg(CJD) mice expressing mutant PrP at a level comparable to that of endogenous PrP in wild-type mice develop a progressive neurological disease that can be easily scored on the basis of kyphosis, foot clasp reflex, unbalanced body posture, and ataxia. Tg(CJD) mice also show sensorimotor deficits, such as inability to climb on a vertically oriented grill and poor performance on a rotarod. These signs are indicative of motor dysfunction, a prominent clinical feature of CJD. No neurological signs are observed in nontransgenic littermates of Tg(CJD) mice or in Tg(WT) mice, strongly indicating that the phenotype is due to expression of the D177N/V128 transgene.

We found that expression of mutant PrP above the endogenous level dramatically exacerbates the Tg(CJD) phenotype. Homozygous mice of the A21 line develop neurological signs much earlier than hemizygous mice (at ~145 versus ~450 days of age) and show much faster disease progression, reaching the terminal stage in ~130 days (Figure 2B). Moreover, the G5 founder, which expressed eight times the endogenous PrP level, died with neurological disease at only 72 days of age, further supporting a direct correlation between D177N/V128 level and disease severity. In contrast, Tg(CJD) lines with PrP expression below the endogenous level remain healthy during their lifetime. This dose-dependent effect of mutant PrP expression has been described in other PrP mutant mice (Chiesa et al., 2000; Nazor et al., 2005; Telling et al., 1996) and supports the concept that higher levels of mutant PrP molecules result in earlier onset and a faster course of disease.

Consistent with the dominant mode of inheritance of CJD^{178} (Goldfarb et al., 1992), expression of wild-type PrP does not rescue the neurological illness of Tg(CJD) mice. Tg(CJD) mice carrying either one or two copies of the endogenous wild-type *Prnp* allele develop neurological signs at an age similar to Tg(CJD)/*Prnp*$^{0/0}$ littermates and invariably progress to terminal disease. Further experiments, however, are necessary to determine whether coexpression of wild-type PrP modifies any other aspects of the Tg(CJD) phenotype, such as the deficits in working memory or the alteration of sleep-wake patterns.

Memory loss is a distinctive early sign of CJD^{178} (Brown et al., 1992). Tg(CJD) mice have a significant deficit in working memory detectable in the eight-arm radial maze well before onset of neurological signs. Tg(CJD) mice appear to be affected specifically in this function since they have no significant alterations in aspects of reference memory as measured by the passive avoidance, object recognition, or Morris water maze tests. Interestingly, Tg(CJD) mice show alterations in calretinin-positive mossy cell terminals of the hippocampus and bipolar interneurons of the cerebral cortex, which are thought to play important roles in spatial orientation and working memory (Crusio and Schwegler, 2005; Wang et al., 2004).

EEG Abnormalities and Sleep Disruption in Tg(CJD) Mice and a CJD^{178} Patient

EEG alterations have been described in CJD since the early 1980s. The alterations depend on the stage of the disease, ranging from nonspecific findings such as diffuse slowing and frontal rhythmic delta activity in the early stage of disease to typical PSWC in the middle and late stages. PSWC has been reported in a carrier of the D178N/V128 mutation (Laplanche et al., 1992) and were also detected in the patient analyzed here.

Tg(CJD) mice develop striking pathological EEG alterations mimicking the human EEG pattern. Bursts of polyphasic complexes and, to a lesser extent, "sawtooth" waves resemble the EEG patterns observed in a feline model of CJD (Gourmelon et al., 1987) and can be regarded as the equivalent of human PSWC (Wieser et al., 2006).

Tg(CJD) mice also exhibit the sleep alterations seen in sporadic CJD (Landolt et al., 2006) and in the CJD^{178} patient described here. The most striking feature is a highly significant reduction of REM sleep during both the light and dark phases of the light-dark cycle in these mice. A second finding is the presence of epochs that cannot be assigned to any normal behavioral state based on standard criteria used for the polygraphic scoring of mouse sleep-wake behavior ("unscored" epochs). The pattern was similar in the CJD^{178} patient, who spent a significant amount of time in a condition that could not be assigned to any normal vigilance or sleep state. A "nonwake-nonsleep" subwakefulness state has been recognized in FFI (Montagna et al., 2003) and in sporadic CJD (Landolt et al., 2006), and we found a severe reduction of sleep efficiency, virtual absence of REM sleep, and absence of usual ultradian modulation in our CJD^{178} patient.

Longitudinal 24 hr monitoring and spectral EEG analysis in FFI patients show that an early and progressive reduction in thalamic sleep spindles and K complexes is an early marker in the natural history of the disease (Cortelli et al., 2006; Montagna et al., 2003); spindling activity was completely absent in the whole 24 hr recording of the CJD^{178} patient described here. Thus, sleep promotion and organization appear to be altered in prion diseases regardless of the specific etiology, suggesting a "continuum" between FFI, CJD^{178}, and sporadic CJD.

The sleep-wake alterations observed in Tg(CJD) mice are not seen in non-Tg littermates and Tg(WT) mice, consistent with these alterations being caused by mutant PrP expression. PrP may regulate circadian rhythm and promote sleep continuity (Tobler et al., 1996), but no significant changes are seen in the percentage of time spent in wakefulness, REM sleep, and NREM sleep in *Prnp*$^{0/0}$ mice. Therefore, the altered sleep-wake behavior of Tg(CJD) mice seen here is unlikely to be due to loss of any putative PrP function in sleep regulation.

Interleukin-1 and tumor necrosis factor are potent inhibitors of REM sleep (Obal and Krueger, 2003). These cytokines are elevated in sporadic and variant CJD and in CJD-infected mice (Kordek et al., 1996; Sharief et al., 1999), suggesting their involvement in the severe REM sleep reduction in Tg(CJD) mice and the CJD^{178} patient.

Neuropathological Features and Biochemical Properties of Mutant PrP in Tg(CJD) Mice

PrP deposition in most forms of prion disease is extracellular, occurring either in typical amyloid plaques or as more diffuse "synaptic-like" deposits in perineuronal and perivacuolar structures throughout the neuropil. In familial CJD linked to the D178N/V129 mutation, weak "synaptic-like" and small focal deposits of PrP are observed (Parchi et al., 2003), and Tg(CJD) mice have the same types of PrP deposits.

A striking pathological alteration in Tg(CJD) mice that appears to be related to PrP deposition is the decrease of calretinin-positive GABAergic neurons in the dentate gyrus of the hippocampus and in layers II and III of the neocortex. In the hippocampus, loss of calretinin is accompanied by reduced synaptophysin staining, suggesting that presynaptic terminals are affected. In the neocortex, the decrease in calretinin is most evident in the neuropil, whereas the cell bodies retain a certain degree of immunoreactivity. These observations suggest that nerve terminals are primarily affected, consistent with the idea that synapses are the main targets of abnormal PrP (Bouzamondo-Bernstein et al., 2004; Jeffrey et al., 2000; Kitamoto et al., 1992).

Specific subpopulations of GABAergic neurons in the hippocampus and cerebral cortex are selectively affected in sporadic CJD and in experimental prion diseases (Guentchev et al., 1997, 1998). In sporadic CJD, parvalbumin-positive interneurons in the frontal cortex are mostly involved, although there is also degeneration of calbindin- and calretinin-positive cells (Belichenko et al., 1999).

In CJD-infected mice, loss of GABAergic inhibitory neurons occurs very early after inoculation, suggesting that it may be an important step during disease development representing the basis of excitatory symptoms (Guentchev et al., 1997, 1998). Whether alterations of calretinin-positive GABAergic neurons in Tg(CJD) mice contribute to the EEG abnormalities observed in this model remains to be established.

Mutant PrP in the brains of Tg(CJD) mice can be distinguished from PrP^C by several biochemical properties, including propensity to form detergent-insoluble aggregates, protease resistance, and reactivity with the 15B3 antibody. D177N/V128 PrP, however, differs from mutant PrP in the brains of CJD^{178} patients because it is much less protease resistant and has a smaller protease-resistant core, suggesting possible structural differences. Experiments to test whether mutant PrP in Tg(CJD) brains is infectious like that in CJD^{178} patients (Brown et al., 1992) are underway.

Impaired Trafficking of Mutant PrP and Its Potential Role in Disease Pathogenesis

We observed that the ER of Tg(CJD) cerebellar granule neurons was dramatically swollen and electron-dense and contained abnormal amounts of mutant PrP. These data suggest that ER retention of mutant PrP may be an instigating pathogenic mechanism in cerebellar granule neurons that could also be active in other neuronal populations.

A number of inherited human diseases are attributable to defects in export of a mutant protein out of the ER (Aridor and Hannan, 2002). In some cases the misfolded mutant protein is triaged by the ER quality control and degraded by the proteasome; in other cases it is retained in the ER lumen and stimulates ER stress response pathways, such as the unfolded protein response (UPR), eventually leading to apoptosis (Kaufman, 1999). We have reported that PrP molecules carrying the D177N mutation are delayed in their biosynthetic maturation in the ER (Drisaldi et al., 2003) but are not subject to retrotranslocation and proteasomal degradation in cerebellar granule neurons (Fioriti et al., 2005). No signs of UPR were detected in the brains of carriers of the D178N/V129 mutation (Unterberger et al., 2006), and we did not find splicing of the mRNA encoding X box-binding protein 1 or increased expression of UPR-regulated genes such as *Grp78/Bip* and *CHOP/GADD153* in the brains of Tg(CJD) mice (data not shown), suggesting that some other pathogenic mechanism may be triggered by this mutation. ER overload with mutant PrP may lead to activation of NF-κB (Pahl and Baeuerle, 1997), with possible consequences for neuronal function and synaptic plasticity (O'Mahony et al., 2006). Alternatively, buildup of the mutant protein in the ER may perturb the ER calcium signaling essential for normal neuronal function (Mattson et al., 2000). Finally, aggregation of mutant PrP in the secretory pathway may interfere with folding, assembly, and transport of other membrane proteins, such as multimeric ion channels or receptors (Schwappach, 2008), leading to defective synaptic transmission.

The fact that Tg(CJD) mice accumulate a misfolded form of mutant PrP in their brains and develop clinical features of CJD argues that essential aspects of pathogenesis are modeled in these animals. Tg(CJD) mice may be suitable for investigating disease mechanisms and testing potential therapies in inherited prion diseases. Since the mutant mice spontaneously develop profound alterations of sleep-wake behavior, they offer a unique model for investigating the pathophysiology of sleep in prion disorders. Finally, comparative studies of Tg(CJD) and transgenic mice expressing other mutant PrPs may provide important information on the cellular and molecular mechanisms responsible for the phenotypic heterogeneity of inherited prion diseases.

EXPERIMENTAL PROCEDURES

Generation of Transgenic Mice

Production of transgenic Tg(WT) mice expressing wild-type PrP tagged with an epitope for the monoclonal antibody 3F4 has been reported previously (Chiesa et al., 1998). In this study, we used hemizygous or homozygous mice of the E1 line, which express two and four times the endogenous PrP level, respectively. The cDNA encoding mouse PrP derived from the $Prnp^a$ allele and containing the 3F4 epitope tag and the D177N and M128V substitutions has been described previously (Fioriti et al., 2005). The coding region of this cDNA was amplified by PCR using Vent polymerase (New England Biolabs) and ligated into the MoPrP.Xho vector, which contains a 12 kb fragment of *Prnp*, including the promoter and intron 1, and drives expression of transgenic PrP in a tissue pattern similar to that of the endogenous protein (Borchelt et al., 1996). Recombinant plasmids were selected by PCR screening and restriction analysis, and their identity was confirmed by sequencing the entire coding region (Chiesa et al., 1998). The transgene was excised by NotI digestion and injected into the pronuclei of fertilized eggs from an F2 cross of C57BL/6J × CBA/J F1 parental mice. Transgenic founders were bred with an inbred colony of Zürich I $Prnp^{0/0}$ mice (C57BL/6J × 129 background) (Bueler et al., 1992; Chiesa et al., 2000). The status of the *Prnp* gene and the presence of the transgene were determined by PCR, and the zygosity of the transgene was determined by Southern blot analysis (Chiesa et al., 1998). The transgenic lines were maintained on the $Prnp^{0/0}$ genotype. For some experiments, the *Prnp* allele was reintroduced by breeding transgenic mice to C57BL/6J × CBA/J mice; nontransgenic $Prnp^{+/+}$ and $Prnp^{0/0}$ littermates were used as controls.

All procedures involving animals and their care were conducted according to European Union (EEC Council Directive 86/609, OJ L 358,1; December 12, 1987) and Italian (D.L. n.116, G.U., suppl. 40; February 18, 1992) laws and policies and in accordance with the United States Department of Agriculture Animal Welfare Act and National Institutes of Health Policy on Humane Care and Use of Laboratory Animals.

Biochemical Analyses

Tissue homogenates were prepared in phosphate-buffered saline (PBS) containing 0.5% NP-40 and 0.5% sodium deoxycholate using a glass/Teflon tissue homogenizer. In some experiments, protease inhibitor cocktail (1 μg/ml pepstatin and leupeptin; 0.5 mM phenylmethylsulfonyl fluoride; 2 mM EDTA) was added to the homogenization buffer. Assays of detergent insolubility, proteinase K (PK) resistance, and immunoprecipitation with antibody 15B3 were carried out as described previously (Biasini et al., 2008; Chiesa et al., 1998; Tremblay et al., 2004). Western blots were developed with monoclonal antibody 3F4 (Kascsak et al., 1987), which selectively recognizes transgenic PrP, or polyclonal antibody P45–66 raised against a synthetic peptide encompassing residues 45–66 of mouse PrP.

Clinical Analysis of Mice

Mice were observed weekly for signs of neurological dysfunction according to a set of objective criteria (Chiesa et al., 1998). Onset of disease was scored as

the time at which at least two of the following neurological signs were observed: foot-clasp reflex, kyphosis, unbalanced body posture, inability to walk on a horizontal metal grid, and inability to remain on a vertical grid for at least 30 s. An accelerating Rota-Rod 7650 (Ugo Basile) was used; mice were first trained twice the week before official testing. They were positioned on the rotating bar and allowed to become acquainted with the environment for 30 s. The rod motor was started at an initial setting of 3 rpm and accelerated to 30 rpm at a constant rate of 0.3 rpm/s for a maximum of 300 s. The performance was scored as latency to fall, in seconds. Animals were given three trials, and the average was used for statistical analysis.

Radial Maze

Spatial working memory was measured using an eight-arm radial maze made of gray plastic with a Plexiglas lid. The arms, which radiated from an octagonal central arena with a diameter of 12 cm, were 30 cm long, 5 cm wide, and 4 cm high. Several external visual cues surrounded the apparatus. Starting one week before testing, the mice were water deprived by being given access to water for only 1 hr per day. One day before starting the task schedule, a habituation trial was run. The mice were placed in the center of the maze and let free to explore the environment for 10 min. The next day, the arms of the radial maze were baited with 50 μl of water. Animals were placed in the center of the maze, and the arm entry sequence was recorded. The task ended once all eight arms of the maze had been visited or after a maximum of 16 trials, whichever came first. Repeated entry into an arm that had already been visited constituted an error. The number of errors and the latency to complete the test were recorded manually by an operator (A.G.) blinded to the experimental groups. Animals were tested for 10 consecutive days.

EEG and Sleep-Wake Behavior

EEG and sleep patterns were investigated in six non-Tg/*Prnp*$^{+/+}$, six non-Tg/*Prnp*$^{0/0}$, six Tg(CJD-A21$^{+/-}$), and five Tg(WT-E1$^{+/+}$) mice. Mice were anesthetized and instrumented for chronic EEG recording according to standard techniques (Baracchi and Opp, 2008) and then allowed at least 10 days to recover from surgery and adapt to the recording conditions. Mice were individually housed in standard cages with food and water ad libitum. Cages were kept in sound-attenuated boxes at a constant temperature between 24.5°C and 26.0°C, with a 12/12 hr light-dark cycle. Gross body activity was detected using an infrared sensor housed in an observation unit that also contained a camera (BIOBSERVE GmbH) allowing continuous recording of the animals' behavior. Movements detected by the infrared sensor were converted to a voltage output. The conditioned EEG signal and the voltage output from the infrared sensor were digitized and collected using custom software (M.R. Opp, University of Michigan). EEG signals and gross body activity were recorded for 24 hr (starting at first light) in undisturbed conditions and used for polygraphic determination of vigilance state. The animals were not handled starting from 48 hr before the recording session. Two mice of different genotypes were randomly matched and recorded simultaneously. The order of recording of mice of the different lines was also randomized.

Postacquisition determination of vigilance state was performed according to standard criteria (Baracchi and Opp, 2008). Visual scoring of 12 s epochs was performed by an investigator (L. Ferrari or S.B.) blinded to the strain. As described in Results, it was sometimes impossible to assign certain epochs to any behavioral state in Tg(CJD) mice. In these cases, epochs were classified as "unscored." EEG power density values were obtained for each animal and each behavioral state by Fourier transform for each artifact-free 12 s scoring epoch for the frequency range 0.5–20 Hz.

Histology

Brains were fixed in Carnoy's fixative (6:3:1 ethanol:chloroform:acetic acid), dehydrated in graded ethanol solutions, cleared in xylene, and embedded in paraffin. Serial sections (5 μm thick) were cut and stained with hematoxylin and eosin, Nissl, or thioflavin S. Some sections were immunostained with rabbit polyclonal anti-glial fibrillary acidic protein (GFAP) (Dako, 1:1000), anti-calretinin (Swant, 1:2000), anti-calbindin (Chemicon, 1:1000), or anti-synaptophysin (Dako, 1:200), followed by visualization with a Vectastain ABC kit (Vector) using 3,3′-diaminobenzidine as chromogen. Alexa 488- or Alexa 546-conjugated secondary antibodies (Molecular Probes Inc.) were used for immunofluorescence.

For PrP immunohistochemistry, sections were incubated with PK (2 μg/ml in 0.1% Brij-35, 50 mM NaCl, 50 mM Tris-HCl [pH 7.8]) for 30 min at room temperature and exposed to guanidine thiocyanate (3 M in H_2O) for 30 min (Giaccone et al., 2000). PK-resistant PrP was detected with monoclonal antibody 3F4 (1:200) (Kascsak et al., 1987) or 12B2 (1:1000) (Langeveld et al., 2006). Results were similar with the two antibodies.

Electron Microscopy

One 269-day-old Tg(WT) mouse, two non-Tg/*Prnp*$^{0/0}$ mice aged 268 and 392 days, two Tg(CJD-A21$^{+/-}$)/*Prnp*$^{0/0}$ mice aged 262 and 488 days, and one 43-day-old Tg(CJD-A21$^{+/+}$)/*Prnp*$^{0/0}$ mouse were deeply anesthetized and perfused through the ascending aorta with PBS (0.1 M; pH 7.4) followed by 4% paraformaldehyde (PFA) and 2.5% glutaraldehyde in PBS. The cerebellum was excised and cut along the sagittal plane with a razor blade, postfixed in 3% glutaraldehyde in PBS, and immersed for 2 hr in OsO_4. After dehydration in a graded series of ethanol, tissue samples were cleared in propylene oxide, embedded in Epon 812 epoxy medium (Fluka), and polymerized at 60°C for 72 hr. From each sample, one semithin section (1 μm) was cut with a Leica EM UC6 ultramicrotome and mounted on glass slides for light microscopic inspection to identify the Purkinje and granular cell layers. Ultrathin sections (70 nm thick) of the area of interest were obtained, counterstained with uranyl acetate and lead citrate, and examined with an energy filter transmission electron microscope (Zeiss LIBRA 120 EFTEM) equipped with a YAG scintillator slow-scan CCD camera.

Immunoelectron Microscopy

Cerebellar granule neurons were prepared from 6-day-old mice as described previously (Fioriti et al., 2005) and cultured for 7 days before immunoelectron microscopy. Cells grown on poly-L-lysine-coated glass coverslips were washed with PBS and fixed in a solution of 4% PFA and 0.1% glutaraldehyde in 0.2 M HEPES buffer (pH 7.4) for 15 min at room temperature. After washing with PBS, cells were incubated for 30 min in blocking solution (50 mM NH_4Cl, 0.1% saponin, 1% BSA in HEPES buffer) and then overnight at 4°C with anti-PrP monoclonal antibody SA65 (Matucci et al., 2005) or 12B2 (Langeveld et al., 2006) diluted 1:250 in blocking solution. Cells were washed and incubated for 1 hr at room temperature with Nanogold-conjugated anti-mouse IgG Fab′ fragment diluted 1:100 in blocking solution and processed according to the Nanogold enhancement protocol (Nanoprobes). Stained cells were embedded in Epon 812 and cut as described previously (Polishchuk et al., 2003). EM images were acquired from thin sections using a Philips Tecnai 12 electron microscope equipped with an ULTRA VIEW CCD digital camera (Philips). Gold particles were quantified in the different compartments of the secretory pathway, and total cell, ER, and Golgi volumes were analyzed using analySIS software (Soft Imaging Systems GmbH). The SA65 and 12B2 antibodies yielded similar results.

Polysomnography

The 24 hr EEG recordings, including complete polysomnography, were taken according to guidelines approved by the Standards of Practice Committee of the American Academy of Sleep Medicine (Kushida et al., 2005). The EEG was acquired with Ag/AgCl electrodes positioned over the vertex and the frontal, central, and occipital regions bilaterally, according to the International 10-20 Electrode Placement System. Two electrooculographic channels, respiratory channels, electrocardiography, bilateral tibialis anterior, and chin electromyography were also recorded. All signals were digitalized at a sampling rate of 256 Hz. The record was visually scored according to standard criteria (Rechtschaffen and Kales, 1968), and the hypnogram was stored digitally, linked to the recording. Arousals, cardiorespiratory events, and EMG activities were recognized by dedicated software and reviewed by a clinical neurophysiologist trained in sleep medicine. A control 24 hr recording was taken in an age-matched healthy subject in the same sleep laboratory.

SUPPLEMENTAL DATA

Supplemental Data can be found online at http://www.neuron.org/supplemental/S0896-6273(08)00755-1.

ACKNOWLEDGMENTS

We thank David Harris for making the transgenic facility of Washington University in St. Louis available to us, for the P45–66 antibody, and for comments on the manuscript. We also thank David Borchelt for the MoPrP.Xho vector, Charles Weissmann for the *Prnp*$^{0/0}$ mice, Richard Kasksak for the 3F4 antibody, Jan P. Langeveld for the 12B2 antibody, Gianluigi Zanusso for the SA65 antibody, and Alex Raeber and Bruno Oesch from Prionics (Zürich) for providing the 15B3 antibody. We are grateful to Roman S. Polishchuk of the Telethon Microscopy and Bio-Imaging Facility (Consorzio Mario Negri Sud) for immunogold staining of cerebellar granule neurons and for useful discussion, to Susanna Mantovani for assistance with animal perfusion and RNA extraction, and to Simona Airaghi for participating in the initial phase of this project. This work was supported by grants from Telethon Italy (TCR05006), "Fondazione Cariplo" and "Compagnia di San Paolo" to R.C., the European Community (QLG-CT-2001-2353 to R.C. and Network of Excellence NeuroPrion to F.T. and R.C.), and the Italian Ministry of Health to F.T. L. Fioriti was supported by a fellowship from the Fondazione Monzino. R.C. is an Assistant Telethon Scientist (Dulbecco Telethon Institute, Fondazione Telethon).

Accepted: September 4, 2008
Published: November 25, 2008

REFERENCES

Aridor, M., and Hannan, L.A. (2002). Traffic jams II: an update of diseases of intracellular transport. Traffic *3*, 781–790.

Baracchi, F., and Opp, M.R. (2008). Sleep-wake behavior and responses to sleep deprivation of mice lacking both interleukin-1 beta receptor 1 and tumor necrosis factor-alpha receptor 1. Brain Behav. Immun. *22*, 982–993.

Belichenko, P.V., Miklossy, J., Belser, B., Budka, H., and Celio, M.R. (1999). Early destruction of the extracellular matrix around parvalbumin-immunoreactive interneurons in Creutzfeldt-Jakob disease. Neurobiol. Dis. *6*, 269–279.

Biasini, E., Seegulam, M.E., Patti, B.N., Solforosi, L., Medrano, A.Z., Christensen, H.M., Senatore, A., Chiesa, R., Williamson, R.A., and Harris, D.A. (2008). Non-infectious aggregates of the prion protein react with several PrP^{Sc}-directed antibodies. J. Neurochem. *105*, 2190–2204.

Borchelt, D.R., Davis, J., Fischer, M., Lee, M.K., Slunt, H.H., Ratovitsky, T., Regard, J., Copeland, N.G., Jenkins, N.A., Sisodia, S.S., and Price, D.L. (1996). A vector for expressing foreign genes in the brains and hearts of transgenic mice. Genet. Anal. *13*, 159–163.

Bouzamondo-Bernstein, E., Hopkins, S.D., Spilman, P., Uyehara-Lock, J., Deering, C., Safar, J., Prusiner, S.B., Ralston, H.J., 3rd, and DeArmond, S.J. (2004). The neurodegeneration sequence in prion diseases: evidence from functional, morphological and ultrastructural studies of the GABAergic system. J. Neuropathol. Exp. Neurol. *63*, 882–899.

Brown, P., Goldfarb, L.G., Kovanen, J., Haltia, M., Cathala, F., Sulima, M., Gibbs, C.J., Jr., and Gajdusek, D.C. (1992). Phenotypic characteristics of familial Creutzfeldt-Jakob disease associated with the codon 178Asn *PRNP* mutation. Ann. Neurol. *31*, 282–285.

Bueler, H., Fischer, M., Lang, Y., Bluethmann, H., Lipp, H.P., DeArmond, S.J., Prusiner, S.B., Aguet, M., and Weissmann, C. (1992). Normal development and behaviour of mice lacking the neuronal cell-surface PrP protein. Nature *356*, 577–582.

Calleja, J., Carpizo, R., Berciano, J., Quintial, C., and Polo, J. (1985). Serial waking-sleep EEGs and evolution of somatosensory potentials in Creutzfeldt-Jakob disease. Electroencephalogr. Clin. Neurophysiol. *60*, 504–508.

Chapman, J., Arlazoroff, A., Goldfarb, L.G., Cervenakova, L., Neufeld, M.Y., Werber, E., Herbert, M., Brown, P., Gajdusek, D.C., and Korczyn, A.D. (1996). Fatal insomnia in a case of familial Creutzfeldt-Jakob disease with the codon 200(Lys) mutation. Neurology *46*, 758–761.

Chiesa, R., and Harris, D.A. (2001). Prion diseases: what is the neurotoxic molecule? Neurobiol. Dis. *8*, 743–763.

Chiesa, R., Piccardo, P., Ghetti, B., and Harris, D.A. (1998). Neurological illness in transgenic mice expressing a prion protein with an insertional mutation. Neuron *21*, 1339–1351.

Chiesa, R., Drisaldi, B., Quaglio, E., Migheli, A., Piccardo, P., Ghetti, B., and Harris, D.A. (2000). Accumulation of protease-resistant prion protein (PrP) and apoptosis of cerebellar granule cells in transgenic mice expressing a PrP insertional mutation. Proc. Natl. Acad. Sci. USA *97*, 5574–5579.

Cortelli, P., Perani, D., Montagna, P., Gallassi, R., Tinuper, P., Federica, P., Avoni, P., Ferrillo, F., Anchisi, D., Moresco, R.M., et al. (2006). Pre-symptomatic diagnosis in fatal familial insomnia: serial neurophysiological and 18FDG-PET studies. Brain *129*, 668–675.

Crusio, W.E., and Schwegler, H. (2005). Learning spatial orientation tasks in the radial-maze and structural variation in the hippocampus in inbred mice. Behav. Brain Funct. *1*, 3.

Drisaldi, B., Stewart, R.S., Adles, C., Stewart, L.R., Quaglio, E., Biasini, E., Fioriti, L., Chiesa, R., and Harris, D.A. (2003). Mutant PrP is delayed in its exit from the endoplasmic reticulum, but neither wild-type nor mutant PrP undergoes retrotranslocation prior to proteasomal degradation. J. Biol. Chem. *278*, 21732–21743.

Fioriti, L., Dossena, S., Stewart, L.R., Stewart, R.S., Harris, D.A., Forloni, G., and Chiesa, R. (2005). Cytosolic prion protein (PrP) is not toxic in N2a cells and primary neurons expressing pathogenic PrP mutations. J. Biol. Chem. *280*, 11320–11328.

Giaccone, G., Canciani, B., Puoti, G., Rossi, G., Goffredo, D., Iussich, S., Fociani, P., Tagliavini, F., and Bugiani, O. (2000). Creutzfeldt-Jakob disease: Carnoy's fixative improves the immunohistochemistry of the proteinase K-resistant prion protein. Brain Pathol. *10*, 31–37.

Goldfarb, L.G., Petersen, R.B., Tabaton, M., Brown, P., LeBlanc, A.C., Montagna, P., Cortelli, P., Julien, J., Vital, C., Pendelbury, W.W., et al. (1992). Fatal familial insomnia and familial Creutzfeldt-Jakob disease: disease phenotype determined by a DNA polymorphism. Science *258*, 806–808.

Gourmelon, P., Amyx, H.L., Baron, H., Lemercier, G., Court, L., and Gibbs, C.J., Jr. (1987). Sleep abnormalities with REM disorder in experimental Creutzfeldt-Jakob disease in cats: a new pathological feature. Brain Res. *411*, 391–396.

Guentchev, M., Hainfellner, J.A., Trabattoni, G.R., and Budka, H. (1997). Distribution of parvalbumin-immunoreactive neurons in brain correlates with hippocampal and temporal cortical pathology in Creutzfeldt-Jakob disease. J. Neuropathol. Exp. Neurol. *56*, 1119–1124.

Guentchev, M., Groschup, M.H., Kordek, R., Liberski, P.P., and Budka, H. (1998). Severe, early and selective loss of a subpopulation of GABAergic inhibitory neurons in experimental transmissible spongiform encephalopathies. Brain Pathol. *8*, 615–623.

Hsiao, K.K., Scott, M., Foster, D., Groth, D.F., DeArmond, S.J., and Prusiner, S.B. (1990). Spontaneous neurodegeneration in transgenic mice with mutant prion protein. Science *250*, 1587–1590.

Jeffrey, M., Halliday, W.G., Bell, J., Johnston, A.R., MacLeod, N.K., Ingham, C., Sayers, A.R., Brown, D.A., and Fraser, J.R. (2000). Synapse loss associated with abnormal PrP precedes neuronal degeneration in the scrapie-infected murine hippocampus. Neuropathol. Appl. Neurobiol. *26*, 41–54.

Kascsak, R.J., Rubenstein, R., Merz, P.A., Tonna-DeMasi, M., Fersko, R., Carp, R.I., Wisniewski, H.M., and Diringer, H. (1987). Mouse polyclonal and monoclonal antibody to scrapie-associated fibril proteins. J. Virol. *61*, 3688–3693.

Kaufman, R.J. (1999). Stress signaling from the lumen of the endoplasmic reticulum: coordination of gene transcriptional and translational controls. Genes Dev. *13*, 1211–1233.

Kazukawa, S., Nakamura, I., Endo, M., Hori, A., and Inao, G. (1987). Serial polysomnograms in Creutzfeldt-Jakob disease. Jpn. J. Psychiatry Neurol. *41*, 651–661.

Kitamoto, T., Shin, R.W., Doh-ura, K., Tomokane, N., Miyazono, M., Muramoto, T., and Tateishi, J. (1992). Abnormal isoform of prion proteins

accumulates in the synaptic structures of the central nervous system in patients with Creutzfeldt-Jakob disease. Am. J. Pathol. *140*, 1285–1294.

Kordek, R., Nerurkar, V.R., Liberski, P.P., Isaacson, S., Yanagihara, R., and Gajdusek, D.C. (1996). Heightened expression of tumor necrosis factor alpha, interleukin 1-alpha, and glial fibrillary acidic protein in experimental Creutzfeldt-Jakob disease in mice. Proc. Natl. Acad. Sci. USA *93*, 9754–9758.

Kushida, C.A., Littner, M.R., Morgenthaler, T., Alessi, C.A., Bailey, D., Coleman, J., Jr., Friedman, L., Hirshkowitz, M., Kapen, S., Kramer, M., et al. (2005). Practice parameters for the indications for polysomnography and related procedures: an update for 2005. Sleep *28*, 499–521.

Landolt, H.P., Glatzel, M., Blattler, T., Achermann, P., Roth, C., Mathis, J., Weis, J., Tobler, I., Aguzzi, A., and Bassetti, C.L. (2006). Sleep-wake disturbances in sporadic Creutzfeldt-Jakob disease. Neurology *66*, 1418–1424.

Langeveld, J.P., Jacobs, J.G., Erkens, J.H., Bossers, A., van Zijderveld, F.G., and van Keulen, L.J. (2006). Rapid and discriminatory diagnosis of scrapie and BSE in retro-pharyngeal lymph nodes of sheep. BMC Vet. Res. *2*, 19.

Laplanche, J.L., Chatelain, J., Thomas, S., Launay, J.M., Gaultier, C., and Derouesne, C. (1992). Uncommon phenotype for a codon 178 mutation of the human PrP gene. Ann. Neurol. *31*, 345.

Mattson, M.P., LaFerla, F.M., Chan, S.L., Leissring, M.A., Shepel, P.N., and Geiger, J.D. (2000). Calcium signaling in the ER: its role in neuronal plasticity and neurodegenerative disorders. Trends Neurosci. *23*, 222–229.

Matucci, A., Zanusso, G., Gelati, M., Farinazzo, A., Fiorini, M., Ferrari, S., Andrighetto, G., Cestari, T., Caramelli, M., Negro, A., et al. (2005). Analysis of mammalian scrapie protein by novel monoclonal antibodies recognizing distinct prion protein glycoforms: an immunoblot and immunohistochemical study at the light and electron microscopic levels. Brain Res. Bull. *65*, 155–162.

Montagna, P., Gambetti, P., Cortelli, P., and Lugaresi, E. (2003). Familial and sporadic fatal insomnia. Lancet Neurol. *2*, 167–176.

Nazor, K.E., Kuhn, F., Seward, T., Green, M., Zwald, D., Purro, M., Schmid, J., Biffiger, K., Power, A.M., Oesch, B., et al. (2005). Immunodetection of disease-associated mutant PrP, which accelerates disease in GSS transgenic mice. EMBO J. *24*, 2472–2480.

Obal, F., Jr., and Krueger, J.M. (2003). Biochemical regulation of non-rapid-eye-movement sleep. Front. Biosci. *8*, d520–d550.

O'Mahony, A., Raber, J., Montano, M., Foehr, E., Han, V., Lu, S.M., Kwon, H., LeFevour, A., Chakraborty-Sett, S., and Greene, W.C. (2006). NF-kappaB/Rel regulates inhibitory and excitatory neuronal function and synaptic plasticity. Mol. Cell. Biol. *26*, 7283–7298.

Pahl, H.L., and Baeuerle, P.A. (1997). The ER-overload response: activation of NF-kappa B. Trends Biochem. Sci. *22*, 63–67.

Parchi, P., Capellari, S., Chen, S.G., and Gambetti, P. (2003). Familial Creutzfeldt-Jakob disease. In Neurodegeneration: The Molecular Pathology of Dementia and Movement Disorders, D.W. Dickson, ed. (Basel, Switzerland: ISN Neuropath Press), pp. 298–306.

Petersen, R.B., Parchi, P., Richardson, S.L., Urig, C.B., and Gambetti, P. (1996). Effect of the D178N mutation and the codon 129 polymorphism on the metabolism of the prion protein. J. Biol. Chem. *271*, 12661–12668.

Polishchuk, E.V., Di Pentima, A., Luini, A., and Polishchuk, R.S. (2003). Mechanism of constitutive export from the golgi: bulk flow via the formation, protrusion, and en bloc cleavage of large trans-golgi network tubular domains. Mol. Biol. Cell *14*, 4470–4485.

Prusiner, S.B. (1998). Prions. Proc. Natl. Acad. Sci. USA *95*, 13363–13383.

Rechtschaffen, A., and Kales, A. (1968). A Manual of Standardized Terminology, Techniques and Scoring System for Sleep Stages in Human Subjects, National Institutes of Health Publication 204 (Washington, DC: US Government Printing Office).

Schwappach, B. (2008). An overview of trafficking and assembly of neurotransmitter receptors and ion channels. Mol. Membr. Biol. *25*, 270–278.

Sharief, M.K., Green, A., Dick, J.P., Gawler, J., and Thompson, E.J. (1999). Heightened intrathecal release of proinflammatory cytokines in Creutzfeldt-Jakob disease. Neurology *52*, 1289–1291.

Taratuto, A.L., Piccardo, P., Reich, E.G., Chen, S.G., Sevlever, G., Schultz, M., Luzzi, A.A., Rugiero, M., Abecasis, G., Endelman, M., et al. (2002). Insomnia associated with thalamic involvement in E200K Creutzfeldt-Jakob disease. Neurology *58*, 362–367.

Telling, G.C., Haga, T., Torchia, M., Tremblay, P., Dearmond, S.J., and Prusiner, S.B. (1996). Interactions between wild-type and mutant prion proteins modulate neurodegeneration in transgenic mice. Genes Dev. *10*, 1736–1750.

Terzano, M.G., Parrino, L., Pietrini, V., Mancia, D., Spaggiari, M.C., Rossi, G., and Tagliavini, F. (1995). Precocious loss of physiological sleep in a case of Creutzfeldt Jakob disease: a serial polygraphic study. Sleep *18*, 849–858.

Tobler, I., Gaus, S.E., Deboer, T., Achermann, P., Fischer, M., Rulicke, T., Moser, M., Oesch, B., McBride, P.A., and Manson, J.C. (1996). Altered circadian activity rhythms and sleep in mice devoid of prion protein. Nature *380*, 639–642.

Tremblay, P., Ball, H.L., Kaneko, K., Groth, D., Hegde, R.S., Cohen, F.E., DeArmond, S.J., Prusiner, S.B., and Safar, J.G. (2004). Mutant PrP^{Sc} conformers induced by a synthetic peptide and several prion strains. J. Virol. *78*, 2088–2099.

Unterberger, U., Hoftberger, R., Gelpi, E., Flicker, H., Budka, H., and Voigtlander, T. (2006). Endoplasmic reticulum stress features are prominent in Alzheimer disease but not in prion diseases in vivo. J. Neuropathol. Exp. Neurol. *65*, 348–357.

Wang, X.J., Tegner, J., Constantinidis, C., and Goldman-Rakic, P.S. (2004). Division of labor among distinct subtypes of inhibitory neurons in a cortical microcircuit of working memory. Proc. Natl. Acad. Sci. USA *101*, 1368–1373.

Wieser, H.G., Schindler, K., and Zumsteg, D. (2006). EEG in Creutzfeldt-Jakob disease. Clin. Neurophysiol. *117*, 935–951.

Young, K., Piccardo, P., Dlouhy, S., Bugiani, O., Tagliavini, F., and Ghetti, B. (1999). The human genetic prion diseases. In Prions: Molecular and Cellular Biology, D.A. Harris, ed. (Wymondham, UK: Horizon Scientific Press), pp. 139–175.